JACS
JOURNAL OF THE AMERICAN CHEMICAL SOCIETY
Article
pubs.acs.org/JACS

High Anhydrous Proton Conductivity of Imidazole-Loaded Mesoporous Polyimides over a Wide Range from Subzero to Moderate Temperature

Yingxiang Ye,[†] Liuqin Zhang,[†] Qinfang Peng,[†] Guan-E Wang,[‡] Yangcan Shen,[†] Ziyin Li,[†] Lihua Wang,[†] Xiuling Ma,[†] Qian-Huo Chen,[†] Zhangjing Zhang,*[,†,‡] and Shengchang Xiang*[,†,§]

[†]College of Chemistry and Chemical Engineering, Fujian Provincial Key Laboratory of Polymer Materials, Fujian Normal University, 32 Shangsan Road, Fuzhou 350007, China

[‡]State Key Laboratory of Structural Chemistry, Fujian Institute of Research on the Structure of Matter, Chinese Academy of Sciences, Fuzhou, Fujian 350002, PR China

[§]College of Life and Environmental Sciences, Minzu University of China, 27 South Zhongguancun Boulevard, Haidian District, Beijing 100081, China

Supporting Information

ABSTRACT: On-board fuel cell technology requires proton conducting materials with high conductivity not only at intermediate temperatures for work but also at room temperature and even at subzero temperature for startup when exposed to the colder climate. To develop such materials is still challenging because many promising candidates for the proton transport on the basis of extended microstructures of water molecules suffer from significant damage by heat at temperatures above 80 °C or by freeze below −5 °C. Here we show imidazole loaded tetrahedral polyimides with mesopores and good stability (Im@Td-PNDI **1** and Im@Td-PPI **2**) exhibiting a high anhydrous proton conductivity over a wide temperature range from −40 to 90 °C. Among all anhydrous proton conductors, the conductivity of **2** is the highest at temperatures below 40 °C and comparable with the best materials, His@[Al(OH)(1,4-ndc)]$_n$ and [$Zn_3(H_2PO_4)_6(H_2O)_3$](Hbim), above 40 °C.

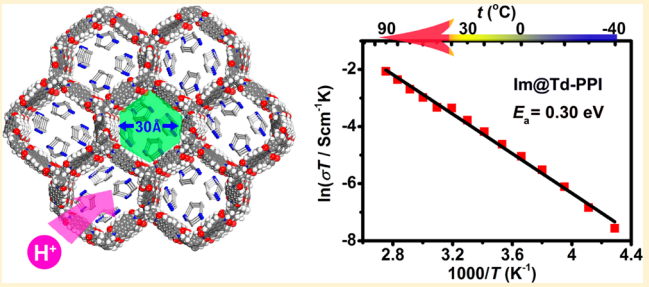

INTRODUCTION

Proton exchange membrane fuel cells (PEMFCs) are very promising as a replacement for traditional engines due to their high power density and ultralow emission features. The state-of-the-art PEMFCs with Nafion as electrolytes can reach a conductivity on the order of 10^{-1}−10^{-2} S cm^{-1} under a limited condition with moderate temperatures (60−80 °C) and high relative humidity (98% RH).[1] Platinum catalysts are necessary for proton exchange membranes (PEMs) under this operating temperature, which will lead to high cost and potential for CO poisoning.[2] In addition, its conductivity will drop significantly above 80 °C due to the loss of inner water, while significant damage to the hydrated PEMs will be induced by freeze/thaw cycles after operation below −5 °C.[3] Much attention has been paid to develop new electrolytes for PEMs able to operate at the temperatures above 80 °C[4−8] but little to develop the PEM electrolytes at subzero temperatures. Therefore, it is desirable but challenging to develop high proton-conductive electrolytes operating over a wide performing temperature range, especially for fuel cells in on-board automotive application: working at moderate temperature and startup at room temperature, even subzero temperature when exposed in the colder climate.

Recently, crystalline porous materials,[9,10] such as metal−organic frameworks (MOFs)/porous coordination polymers (PCPs) and covalent organic frameworks (COFs), show tremendous possibilities to be candidates for electrolytes and for better understanding of proton conduction in diverse structures.[11] Their designable framework structures and high surface areas provide great opportunities to orderly accommodate proton carriers as well as to systemically modify the concentration and mobility of proton carriers in pores. Many porous MOFs with hydrated water could possess interesting proton conducting properties at moderate temperature and high humidification.[12−15] For the purpose of a higher temperature (>80 °C) operation system without dependency on humidity variations, non-water-media molecules, including nonvolatile acids[16] (such as H_2SO_4 and H_3PO_4) and organic aryl molecules[4−7] (such as triazole and imidazole), have been introduced into pores of MOFs to form anhydrous proton carrier pathways. Among them, H_2SO_4@MIL-101 achieved the highest σ value of 1×10^{-2} S·cm^{-1} at 150 °C under very low humidity (0.13% RH).[16] [$Zn_3(H_2PO_4)_6(H_2O)_3$](Hbim) and

Received: November 5, 2014
Published: December 30, 2014

DOI: 10.1021/ja511389q
J. Am. Chem. Soc. 2015, 137, 913−918

Scheme 1. Synthesis Routes to Im@Td-PNDI and Im@Td-PPI

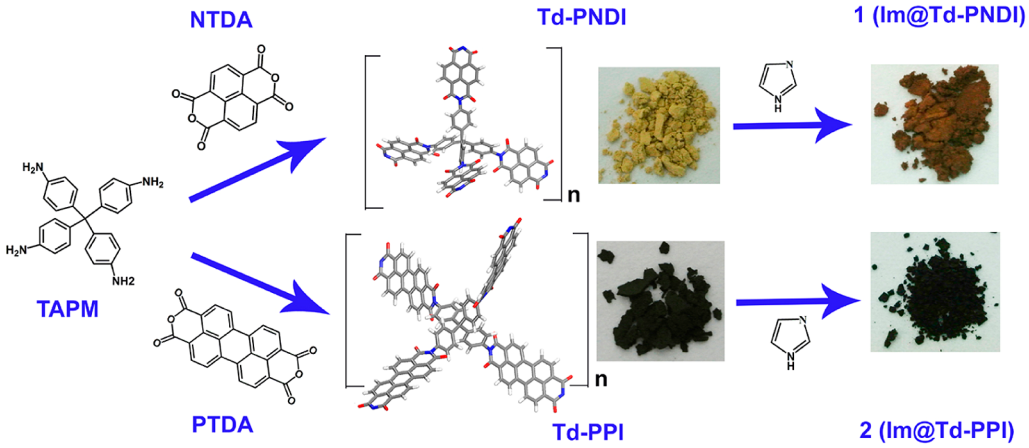

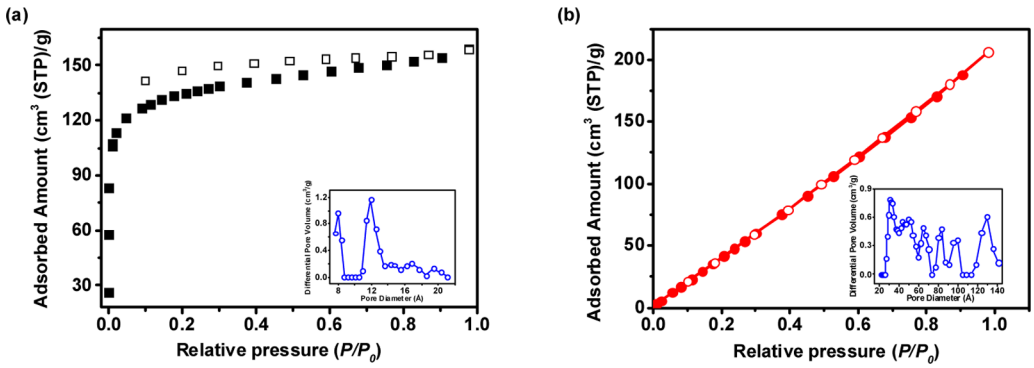

Figure 1. N_2 sorption isotherms of (a) Td-PNDI and (b) Td-PPI at 77 K. Solid and open symbols represent adsorption and desorption, respectively. (Inset) Pore size distributions of (a) Td-PNDI and (b) Td-PPI calculated by the NLDFT method.

His@$[Al(OH)(1,4\text{-ndc})]_n$ presented intrinsic anhydrous proton conductivity as high as 1.3×10^{-3} S cm^{-1} at 120 °C and 1.7×10^{-3} S cm^{-1} at 150 °C,[4a,6a] respectively. However, poor hydrolytic stability of the coordination bonds and the framework backbone of MOFs limit their industrial applicability under fuel cell operating conditions. Covalent organic frameworks (COFs),[17] being one type of porous polymers, resemble perfect crystalline organic analogues to the MOFs.[18] Research work on proton conducting COFs is still in its infancy because they suffer from chemical and hydrothermal instability, and only specially designed monomers can enhance their stability.[19] To date, only one example, H_3PO_4@Tp-Azo, has been tested and shows proton conducting behaviors under both hydrous and anhydrous conditions (9.9×10^{-4} and 6.7×10^{-5} S cm^{-1}, respectively).[20] Its anhydrous proton conductivity reaches a maximum around 59−67 °C and then decreases gradually upon increasing temperature. Thus, it is crucial to explore new porous materials with good stability and proton-conducting performance under different working conditions.

In this paper, the strategy through loading imidazole carriers into mesoporous polyimides is proposed to realize the first examples of porous organic polymers (POPs based proton conductors (Im@Td-PNDI **1** and Im@Td-PPI **2**) operating over a wide temperature range from subzero to moderate temperatures above 80 °C, under the following considerations: (1) Imidazole (Im) is chosen as the proton transfer agent because it shows fast proton transfer behavior and an amphiprotic nature, analogous to that of water.[5] Superior to water media, imidazole with high melting and boiling points will support a more stable proton-transport pathway in a wide temperature range. (2) The tetrahedral polyimides (Td-PNDI and Td-PPI) show robust frameworks, good thermal and hydrolytic stability even when exposed to aqueous and acidic conditions,[21,22] and designable large mesopores favoring an increase in the moving freedom of proton carriers to achieve good proton conducting characteristics, while all hosts reported for the proton conductor with imdazole carriers are microporous coordination polymers.[5] (3) These POPs without metal ions may be more electrochemically stable in comparison with MOFs.

RESULTS AND DISCUSSION

The imidazole-loaded proton-conducting POP materials **1** and **2** were prepared by vaporizing imidazoles into the solvent-free polyimides Td-PNDI and Td-PPI at 120 °C for 36 h. As shown in Scheme 1, Td-PNDI and Td-PPI are both constructed from the condensation of tetrahedral building blocks tetrakis(4-aminophenyl)-methane (TAPM) and rigid dianhydride linkers, perylene dianhydride (PTDA) linker in Td-PPI, instead of naphthalene dianhydride (NTDA) in Td-PNDI. Solvent-free Td-PNDI has been confirmed to be permanently porous and robust.[21a] Computational simulations have been used previously to predict or rationalize the amorphous structures of Td-PNDI and Td-PPI with a diamond topology.[23] The permanent porosity of solvent-free polyimide networks in Td-PNDI and Td-PPI was evaluated by the N_2 adsorption isotherm at 77 K. As illustrated in Figure 1, Td-PNDI shows a type-I sorption behavior typical for microporous materials

DOI: 10.1021/ja511389q
J. Am. Chem. Soc. 2015, 137, 913−918

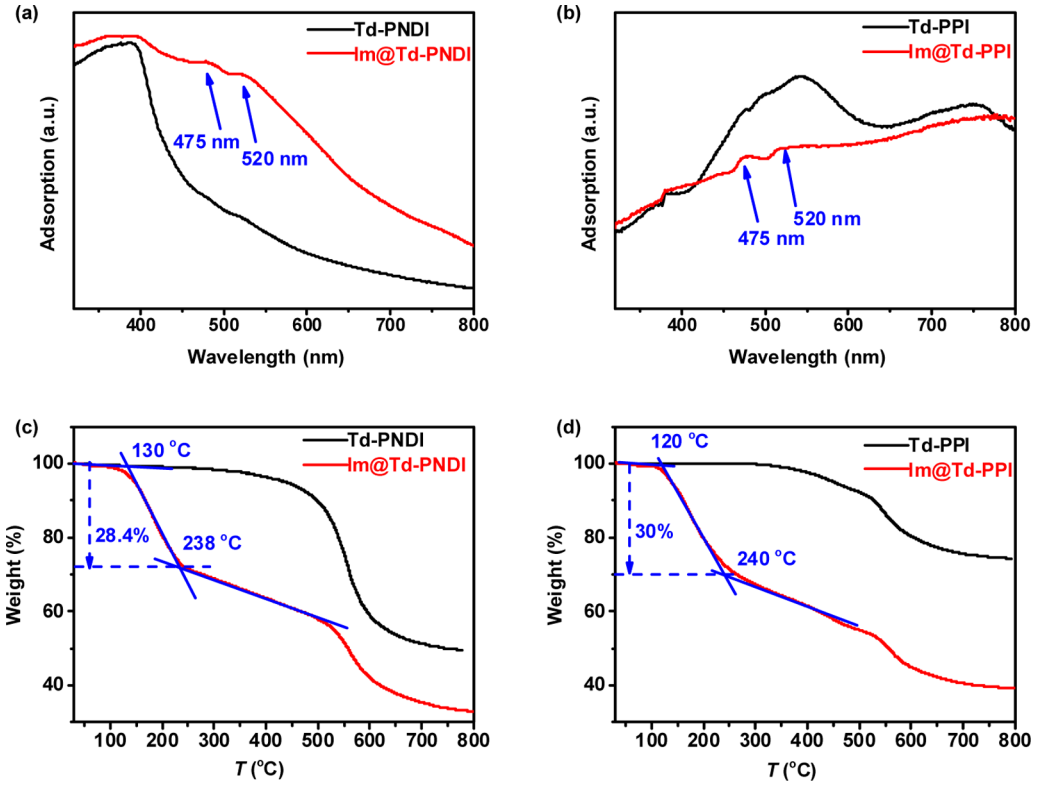

Figure 2. Solid-state UV−vis absorption spectra (a, b) and TGA curves (c, d) of polyimides (black) and imidazole loaded polyimides (red).

with a Brunauer−Emmett−Teller (BET) surface area of 465 m^2 g^{-1}, while the isotherm of Td-PPI is typical of Henry linear adsorption for mesoporous structures with a BET surface area of 325 m^2/g. The single point pore volume at P/P_o of 0.97 for Td-PNDI and Td-PPI are 0.245 and 0.319 cm^3/g, respectively. The differential pore volume distributions for both polymers are calculated using the nonlocal density functional theory (NLDFT) method. The major pores in Td-PNDI locate at around 0.8 and 1.2 nm, while Td-PPI has a wide pore-size distribution in the mesopore region ranging from 3 to 13 nm, indicating that Td-PPI has a larger space than Td-PNDI to hold up imidazole molecules (4.3 × 3.7 $Å^2$).

It is essential to examine the existence of imidazole molecules in the pores of polyimide, rather than aggregation on the outer surface, which has been confirmed by solid-state FT-IR spectra, UV−vis absorption spectra, powder X-ray diffraction (PXRD), scanning electron microscope (SEM), and TGA and DSC profiles in Figure 2 and Figures S2−S5 (Supporting Information). SEM images show no obvious change in the surfaces of **1** and **2** in comparison with their own parent POP materials, indicating imidazole molecules entered into pores of polyimide frameworks without being aggregated on the outer surface of polyimides (Figure S2, Supporting Information). PXRD measurements of polyimides reveal broad peaks, implying that both polyimides are amorphous, and the presence of several peak maxima in the diffractogram indicates the locally ordered nature of these networks (Figure S3, Supporting Information).[21,22] After imidazole was loaded, **1** and **2** presented the same angle peaks with polyimide powders. Solid-state FT-IR spectra of the initial monomers and polyimides are presented in Figure S4 (Supporting Information). In the imidazole loaded polyimides, the weak absorption at around 3140 cm^{-1} could be attributed to the unsaturated C−H stretching vibrations of imidazole molecules. The absorption bands around 1053 cm^{-1} agree well with the C−N stretching vibrations of imidazole in the compounds. The FT-IR spectral information indicated the imidazole molecules were successfully loaded in the polyimide frameworks. After imidazole was vaporized into guest-free Td-PNDI and Td-PPI at 120 °C for 36 h, obvious color changes were observed from tan to red-brown for **1** and from dark green to dark red for **2**, respectively. Correspondingly, two new peaks appearing at around 475 and 520 nm, respectively, in the UV−vis absorption spectra of **1** and **2** are not observed in the spectra of imidazole[24] or polyimides (Td-PNDI and Td-PPI), which can be attributed to the host−guest interactions between the host POP frameworks and the guest imidazole molecules (Figure 2a,b).

TGA measurements were carried out to examine the thermal stability of the porous networks (Figure 2c,d). Both parent polyimide frameworks are stable up to 500 °C. The thermogravimetric profiles show 28.4% weight imidazole loading or 4.9 imidazole/1 TAPM for **1**, and 30% weight or 6.9 imidazole/1 TAPM for **2**. The release of accommodated imidazole in **1** starts at 130 °C and finishes at 238 °C, and the release in **2** begins at 120 °C and finishes at 240 °C. The lower starting temperature in **2** implies that the imidazole guests have less interaction with Td-PPI hosts, and thus may have higher mobility in **2**, in contrast with those in **1**. Considering that the dispersion of imidazole is uniform in the pores, the density of imidazole loaded in the pores could be calculated from the single point pore volumes of the hosts. The values are 1.15 and 0.94 g/cm^3 for **1** and **2**, respectively, lower than 1.23 g/cm^3 for bulk imidazole solid at ambient temperature,[25] indicating that the loaded imidazole molecules in polyimide frameworks have a different packing arrangement with bulk imidazole. It is further confirmed by the DSC profiles in Figure S5 (Supporting Information). For the bulk imidazole, it shows a sharp exothermic peak at the melting temperature (93 °C), while

DOI: 10.1021/ja511389q
J. Am. Chem. Soc. 2015, 137, 913−918

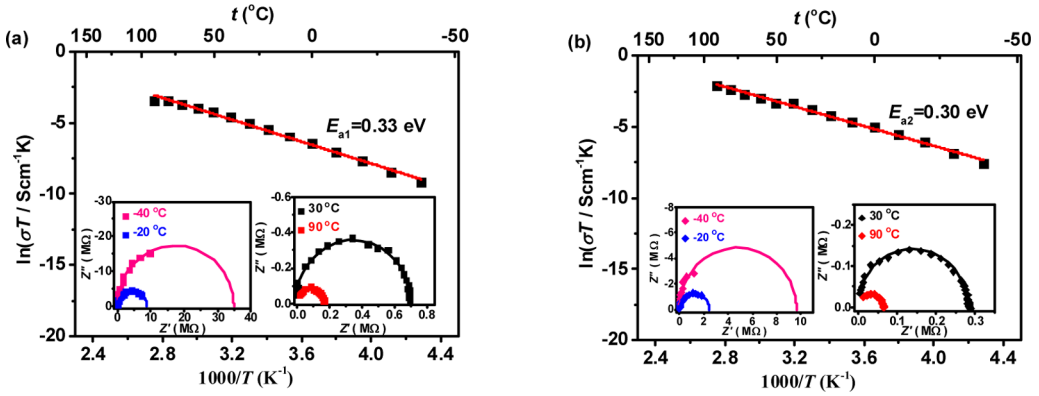

Figure 3. Arrhenius plots for **1** (a) and **2** (b) under anhydrous conditions. Least-squares fitting is shown as a solid line. (Inset) Typical Nyquist plots of **1** and **2** under anhydrous conditions at different temperatures.

the imidazole loaded **1** and **2** do not present a clear peak from room temperature to 120 °C, suggesting that the accommodated imidazole does not undergo phase transition in the temperature range measured.

Temperature-dependent proton conductivities of solvent-free polyimides (Td-PNDI and Td-PPI) and imidazole loaded polymers (**1** and **2**) were measured by using AC impedance spectroscopy under anhydrous conditions. No semicircle was observed in Td-PNDI and Td-PPI, which is indicative of negligible proton conductivity for these parent polyimide frameworks. The existence of imidazoles leads to typical proton conductivities of **1** and **2**, determined from the semicircles in the Nyquist plots, as shown in Figure 3 and Figures S6 and S7 (Supporting Information). The proton conductivity of **2** is higher than that of **1** over the temperature range from −40 to 90 °C, which can be attributed to the lower density and higher mobility of imidazole guests accommodated in the larger mesopore of Td-PPI. The comparison of the conductivities of **1** and **2** with some representative MOF and COF materials under anhydrous conditions is shown in Figure 4, Figure S8

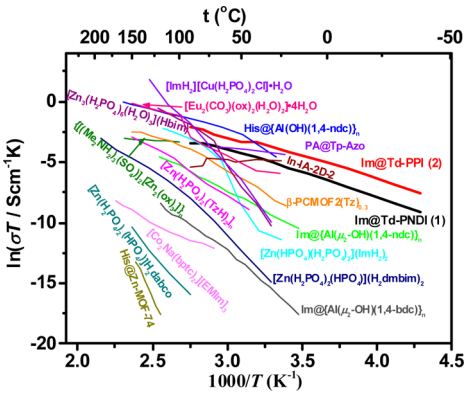

Figure 4. Arrhenius plot for **1** and **2** in comparison with other representative proton-conducting MOFs and COF materials under anhydrous conditions.

(Supporting Information), and Table S2 (Supporting Information). Anhydrous proton conductivities for most of the MOF and COF materials reported are remarkably reduced below room temperature, similar to the hydrated PEMs suffering from significant damage by freeze. Even under subzero temperature (−40 °C), obvious proton conductivity for **1** and **2** has been observed with respective values of 4.58×10^{-7} and 2.23×10^{-6} S cm^{-1}, which has never been shown in crystalline porous materials. It can be contributed from imidazole molecules with high melting points. Upon heating, their conductivity values gradually increase to 2.26×10^{-5} S cm^{-1} for **1** and 7.64×10^{-5} S cm^{-1} for **2** at ambient temperature (30 °C), much higher than the values for solid bulk imidazole (10^{-8} S cm^{-1})[5a] as well as for other imidazole loaded microporous materials (3.3×10^{-8} and 5.5×10^{-8} S cm^{-1} for $[Zn(HPO_4)(H_2PO_4)_2]$ and $[Al(\mu_2\text{-}OH)(1,4\text{-ndc})]$, respectively).[5a,b] The value of **2** is the highest among all reported anhydrous proton conductors under these working conditions (Figure 4 and Figure S8, Supporting Information).[4−8,13f,20] Until a temperature of 90 °C, their conductivity values reach a maximum of 9.04×10^{-5} S cm^{-1} for **1** and 3.49×10^{-4} S cm^{-1} for **2**, respectively, which is comparable to $[ImH_2][Cu(H_2PO_4)_2Cl]\cdot H_2O$ (5.12×10^{-4} S cm^{-1})[5c] and higher than other imidazole-impregnated MOFs. In particular, the value of **2** at 90 °C is comparable with the highest values (7.02×10^{-4} S cm^{-1} for His@$[Al(OH)(1,4\text{-ndc})]_n$[4a] and 4.18×10^{-4} S cm^{-1} for $Zn_3(H_2PO_4)_6(H_2O)_3(Hbim)$)[6a] among the anhydrous proton conducting MOF and COF materials reported to date. Moreover, the proton conductivity of **2** within the temperature range from room temperature to 90 °C is the highest among all imidazole incorporated porous materials without the contributions from lattice water.[5c] This may possibly be due to the large space provided by the mesopores in **2** favors to the movements of the imidazole then to improve the proton mobility. On the basis of the Arrhenius equation (Figure 3), the activation energy of **1** and **2** is 0.33 and 0.30 eV, respectively, clearly smaller than the reported anhydrous imidazole-loaded MOFs.[5] The low activation energy reflects the Grotthuss mechanism of proton conduction for **1** and **2**.[12a,e] Notably, the observation of the high proton conductivity and low energy values of **2** in the temperature range from 40 to 90 °C suggests that it belongs to anhydrous fast-ion conductors.[12a]

CONCLUSIONS

In conclusion, the strategy based on tetrahedral polyimides (Td-PNDI and Td-PPI) with controllable mesopores and good stability via imidazole loading is proposed to realize the first examples of porous organic polymer (POP) materials (Im@Td-PNDI **1** and Im@Td-PPI **2**) with high anhydrous proton conductivity over a wide temperature range from subzero to 90 °C. Obvious proton conducting capability at low temperature down to −40 °C for **1** and **2** has never been shown in other MOF or COF materials. Td-PPI has larger mesopores than Td-

DOI: 10.1021/ja511389q
J. Am. Chem. Soc. 2015, 137, 913−918

PNDI to accommodate the imidazole guests with the lower density and higher mobility, resulting in the higher proton conductivity for **2**. The conductivity reaches a maximum (9.04×10^{-5} S cm^{-1} for **1** and 3.49×10^{-4} S cm^{-1} for **2**) at 90 °C. Among all anhydrous proton conductors, the conductivity of **2** is the highest at the temperatures below 40 °C, and **2** belongs to anhydrous fast-ion conductors in the temperature range from 40 to 90 °C with the values comparable with those for the best materials, His@[Al(OH)(1,4-ndc)]$_n$ and $[Zn_3(H_2PO_4)_6(H_2O)_3]$(Hbim). We will continue working on the design of new POP-based proton conducting materials and their fuel cell applications. We believe that our findings will encourage further work in subzero-temperature proton conducting materials in the near future.

EXPERIMENTAL SECTION

Preparation of Imidazole-Loaded Frameworks. After syntheses of TAPM, Td-PNDI, and Td-PPI (Supporting Information), Td-PNDI and Td-PPI were finely grounded and then degassed by heating to 120 °C under reduced pressure for 12 h to remove guest molecules. Imidazole was vaporized into guest-free Td-PNDI (0.151 g) and Td-PPI (0.151 g) at 120 °C for 36 h to yield **1** and **2**. The amount of loaded imidazole was determined by thermogravimetric analysis.

Proton Conductivity Measurement of 1 and 2. The samples for conductivity measurements were added to a homemade cylindrical closed glass container with an inner diameter of 0.4 cm and connected between two stainless steel electrodes. The sample thickness of 2.00 and 2.70 cm, respectively, for **1** and **2** was measured using a vernier caliper.

Measurements were performed using an impedance and gain-phase analyzer (Solartron analytical ModuLab 126) over a frequency range from 100 Hz to 1 MHz with an input voltage amplitude of 100 mV. The measurement closed glass container was flushed with dry N_2 before measurement to remove moisture. The closed glass container was heated up to 90 °C for a few minutes to make the arrangement of imidazole molecules regularly oriented. Measurements were taken under anhydrous conditions and done at thermal equilibrium by holding for 30 min in the temperature range from −40 to 90 °C. Proton conductivity was calculated using the following equation

$$\sigma = \frac{l}{SR_s} \tag{1}$$

where l and S are the length (cm) and cross-sectional area (cm^2) of the samples, respectively, and R_s, which was extracted directly from the impedance plots, is the bulk resistance of the sample (Ω). The activation energy (E_a) for the materials conductivity was estimated from the following equation

$$\sigma T = \sigma_0 \exp\left(-\frac{E_a}{k_B T}\right) \tag{2}$$

where σ is the ionic conductivity, σ_0 is the preexponential factor, k_B is the Boltzmann constant, and T is the temperature. ZView software was used to extrapolate impedance data results by means of an equivalent circuit simulation to complete the Nyquist plot and obtain the resistance values.

ASSOCIATED CONTENT

Supporting Information

Detailed information regarding the experimental methods and procedures, and supportive figures and tables. This material is available free of charge via the Internet at http://pubs.acs.org.

AUTHOR INFORMATION

Corresponding Authors

*zzhang@fjnu.edu.cn
*scxiang@fjnu.edu.cn

Notes

The authors declare no competing financial interest.

ACKNOWLEDGMENTS

This work was financially supported by the National Natural Science Foundation of China (21207018, 21273033, and 21203024) and the Fujian Science and Technology Department (2014J06003). S.X. gratefully acknowledges the support of the Recruitment Program of Global Young Experts, Program for New Century Excellent Talents in University (NCET-10-0108), and the Award "MinJiang Scholar Program" in Fujian Province.

REFERENCES

(1) Paddison, S. J. *Annu. Rev. Mater. Res.* **2003**, *33*, 289.

(2) Li, Q.; He, R.; Jensen, J. O.; Bjerrum, N. J. *Chem. Mater.* **2003**, *15*, 4896.

(3) (a) Yan, Q.; Toghiani, H.; Lee, Y.-W.; Liang, K.; Causey, H. *J. Power Sources* **2006**, *160*, 1242. (b) Kim, S.; Mench, M. M. *J. Power Sources* **2007**, *174*, 206. (c) Song, M.-K.; Li, H.; Li, J.; Zhao, D.; Wang, J.; Liu, M. *Adv. Mater.* **2014**, *26*, 1277.

(4) (a) Umeyama, D.; Horike, S.; Inukai, M.; Hijikata, Y.; Kitagawa, S. *Angew. Chem., Int. Ed.* **2011**, *50*, 11706. (b) Inukai, M.; Horike, S.; Umeyama, D.; Hijikatab, Y.; Kitagawa, S. *Dalton Trans.* **2012**, *41*, 13261.

(5) (a) Bureekaew, S.; Horike, S.; Higuchi, M.; Mizuno, M.; Kawamura, T.; Tanaka, D.; Yanai, N.; Kitagawa, S. *Nat. Mater.* **2009**, *8*, 831. (b) Horike, S.; Umeyama, D.; Inukai, M.; Itakura, T.; Kitagawa, S. *J. Am. Chem. Soc.* **2012**, *134*, 7612. (c) Horike, S.; Chen, W.; Itakura, T.; Inukai, M.; Umeyama, D.; Asakura, H.; Kitagawa, S. *Chem. Commun.* **2014**, *50*, 10241.

(6) (a) Umeyama, D.; Horike, S.; Inukai, M.; Kitagawa, S. *J. Am. Chem. Soc.* **2013**, *135*, 11345. (b) Inukai, M.; Horike, S.; Chen, W.; Umeyama, D.; Itakura, T.; Kitagawa, S. *J. Mater. Chem. A* **2014**, *2*, 10404.

(7) (a) Hurd, J. A.; Vaidhyanathan, R.; Thangadurai, V.; Ratcliffe, C. I.; Moudrakovski, I. L.; Shimizu, G. K. H. *Nat. Chem.* **2009**, *1*, 705. (b) Umeyama, D.; Horike, S.; Inukai, M.; Itakura, T.; Kitagawa, S. *J. Am. Chem. Soc.* **2012**, *134*, 12780.

(8) Tang, Q.; Liu, Y.; Liu, S.; He, D.; Miao, J.; Wang, X.; Yang, G.; Shi, Z.; Zheng, Z. *J. Am. Chem. Soc.* **2014**, *136*, 12444.

(9) (a) O'Keeffe, M.; Yaghi, O. M. *Chem. Rev.* **2012**, *112*, 675. (b) Zhou, H. C.; Long, J. R.; Yaghi, O. M. *Chem. Rev.* **2012**, *112*, 673. (c) Li, J. R.; Sculley, J.; Zhou, H. C. *Chem. Rev.* **2012**, *112*, 869. (d) Cui, Y.; Yue, Y.; Qian, G.; Chen, B. *Chem. Rev.* **2012**, *112*, 1126. (e) Zhou, H. C.; Kitagawa, S. *Chem. Soc. Rev.* **2014**, *43*, 5415. (f) Zhu, Q. L.; Xu, Q. *Chem. Soc. Rev.* **2014**, *43*, 5468. (g) Lu, W.; Wei, Z.; Gu, Z. Y.; Liu, T. F.; Park, J.; Tian, J.; Zhang, M.; Zhang, Q.; Gentle, T., III; Bosch, M.; Zhou, H. C. *Chem. Soc. Rev.* **2014**, *43*, 5561.

(10) (a) Zhang, Z.-J.; Yao, Z.-Z.; Xiang, S.-C.; Chen, B. *Energy Environ. Sci.* **2014**, *7*, 2868. (b) Xiang, S.-C.; He, Y.; Zhang, Z.-J.; Wu, H.; Zhou, W.; Krishna, R.; Chen, B. *Nat. Commun.* **2012**, *3*, 954. (c) Xiang, S.-C.; Zhang, Z.-J.; Zhao, C.-G.; Hong, K.-L.; Zhao, X.-B.; Ding, D.; Xie, M.; Wu, C.-D.; Das, M. C.; Gill, R.; Thomas, K. M.; Chen, B. *Nat. Commun.* **2011**, *2*, 204. (d) Xiang, S.-C.; Zhou, W.; Zhang, Z.-J.; Green, M. A.; Liu, Y.; Chen, B. *Angew. Chem., Int. Ed.* **2010**, *49*, 4615. (e) Xiang, S.-C.; Zhou, W.; Gallegos, J. M.; Liu, Y.; Chen, B. *J. Am. Chem. Soc.* **2009**, *131*, 12415. (f) Xiang, S.-C.; Wu, X.-T.; Zhang, J.-J.; Hu, S.-M.; Fu, R.-B.; Zhang, X.-D. *J. Am. Chem. Soc.* **2005**, *127*, 16352.

(11) (a) Yoon, M.; Suh, K.; Natarajan, S.; Kim, K. *Angew. Chem., Int. Ed.* **2013**, *52*, 2688. (b) Horike, S.; Umeyama, D.; Kitagawa, S. *Acc. Chem. Res.* **2013**, *46*, 2376. (c) Yamada, T.; Otsubo, K.; Makiurac, R.;

DOI: 10.1021/ja511389q
J. Am. Chem. Soc. 2015, 137, 913−918

Kitagawa, H. *Chem. Soc. Rev.* **2013**, *42*, 6655. (d) Li, S.-L.; Xu, Q. *Energy Environ. Sci.* **2013**, *6*, 1656. (e) Shimizu, G. K. H.; Taylor, J. M.; Kim, S. R. *Science* **2013**, *341*, 354. (f) Ramaswamy, P.; Wong, N. E.; Shimizu, G. K. H. *Chem. Soc. Rev.* **2014**, *43*, 5913. (g) Canivet, J.; Fateeva, A.; Guo, Y.; Coasne, B.; Farrusseng, D. *Chem. Soc. Rev.* **2014**, *43*, 5594.

(12) (a) Yamada, T.; Sadakiyo, M.; Kitagawa, H. *J. Am. Chem. Soc.* **2009**, *131*, 3144. (b) Sadakiyo, M.; Yamada, T.; Kitagawa, H. *J. Am. Chem. Soc.* **2009**, *131*, 9906. (c) Ōkawa, H.; Shigematsu, A.; Sadakiyo, M.; Miyagawa, T.; Yoneda, K.; Ohba, M.; Kitagawa, H. *J. Am. Chem. Soc.* **2009**, *131*, 13516. (d) Yamada, T.; Morikawa, S.; Kitagawa, H. *Bull. Chem. Soc. Jpn.* **2010**, *83*, 42. (e) Shigematsu, A.; Yamada, T.; Kitagawa, H. *J. Am. Chem. Soc.* **2011**, *133*, 2034. (f) Sadakiyo, M.; Ōkawa, H.; Shigematsu, A.; Ohba, M.; Yamada, T.; Kitagawa, H. *J. Am. Chem. Soc.* **2012**, *134*, 5472. (g) Sen, S.; Nair, N. N.; Yamada, T.; Kitagawa, H.; Bharadwaj, P. K. *J. Am. Chem. Soc.* **2012**, *134*, 19432. (h) Xu, G.; Otsubo, K.; Yamada, T.; Sakaida, S.; Kitagawa, H. *J. Am. Chem. Soc.* **2013**, *135*, 7438. (i) Sadakiyo, M.; Yamada, T.; Honda, K.; Matsui, H.; Kitagawa, H. *J. Am. Chem. Soc.* **2014**, *136*, 7701. (j) Sadakiyo, M.; Yamada, T.; Kitagawa, H. *J. Am. Chem. Soc.* **2014**, *136*, 13166. (k) Yamada, T.; Shirai, Y.; Kitagawa, H. *Chem.—Asian J.* **2014**, *9*, 1316.

(13) (a) Sahoo, S. C.; Kundu, T.; Banerjee, R. *J. Am. Chem. Soc.* **2011**, *133*, 17950. (b) Dey, C.; Kundu, T.; Banerjee, R. *Chem. Commun.* **2012**, *48*, 266. (c) Kundu, T.; Sahoo, S. C.; Banerjee, R. *Chem. Commun.* **2012**, *48*, 4998. (d) Panda, T.; Kunduz, T.; Banerjee, R. *Chem. Commun.* **2012**, *48*, 5464. (e) Mallick, A.; Kundu, T.; Banerjee, R. *Chem. Commun.* **2012**, *48*, 8829. (f) Panda, T.; Kundu, T.; Banerjee, R. *Chem. Commun.* **2013**, *49*, 6197.

(14) (a) Taylor, J. M.; Mah, R. K.; Moudrakovski, I. L.; Ratcliffe, C. I.; Vaidhyanathan, R.; Shimizu, G. K. H. *J. Am. Chem. Soc.* **2010**, *132*, 14055. (b) Taylor, J. M.; Dawson, K. W.; Shimizu, G. K. H. *J. Am. Chem. Soc.* **2013**, *135*, 1193. (c) Kim, S.; Dawson, K. W.; Gelfand, B. S.; Taylor, J. M.; Shimizu, G. K. H. *J. Am. Chem. Soc.* **2013**, *135*, 963. (d) Meng, X.; Song, X.-Z.; Song, S.-Y.; Yang, G.-C.; Zhu, M.; Hao, Z.-M.; Zhao, S.-N.; Zhang, H.-J. *Chem. Commun.* **2013**, *49*, 8483. (e) Ramaswamy, P.; Matsuda, R.; Kosaka, W.; Akiyama, G.; Jeona, H. J.; Kitagawa, S. *Chem. Commun.* **2014**, *50*, 1144. (f) Zhu, M.; Hao, Z.-M.; Song, X.-Z.; Meng, X.; Zhao, S.-N.; Song, S.-Y.; Zhang, H.-J. *Chem. Commun.* **2014**, *50*, 1912.

(15) (a) Sadakiyo, M.; Kasai, H.; Kato, K.; Takata, M.; Yamauchi, M. *J. Am. Chem. Soc.* **2014**, *136*, 1702. (b) Phang, W. J.; Lee, W. R.; Yoo, K.; Ryu, D. W.; Kim, B. S.; Hong, C. S. *Angew. Chem., Int. Ed.* **2014**, *53*, 8523. (c) Wang, R.; Dong, X.-Y.; Xu, H.; Pei, R.-B.; Ma, M.-L.; Zang, S.-Q.; Hou, H.-W.; Mak, T. C. W. *Chem. Commun.* **2014**, *50*, 9153. (d) Mao, C.; Kudla, R. A.; Zuo, F.; Zhao, X.; Mueller, L. J.; Bu, X.; Feng, P. *J. Am. Chem. Soc.* **2014**, *136*, 7579. (e) Gassensmith, J. J.; Kim, J. Y.; Holcroft, J. M.; Farha, O. K.; Stoddart, J. F.; Hupp, J. T.; Jeong, N. C. *J. Am. Chem. Soc.* **2014**, *136*, 8277. (f) Dong, X.-Y.; Wang, R.; Wang, J.-Z.; Zang, S.-Q.; Mak, T. C. W. *J. Mater. Chem. A* **2015**, *3*, 641.

(16) Ponomareva, V. G.; Kovalenko, K. A.; Chupakhin, A. P.; Dybtsev, D. N.; Shutova, E. S.; Fedin, V. P. *J. Am. Chem. Soc.* **2012**, *134*, 15640.

(17) (a) Wu, D.; Xu, F.; Sun, B.; Fu, R.; He, H.; Matyjaszewski, K. *Chem. Rev.* **2012**, *112*, 3959. (b) Feng, X.; Ding, X.; Jiang, D. *Chem. Soc. Rev.* **2012**, *41*, 6010.

(18) (a) Ding, S.-Y.; Wang, W. *Chem. Soc. Rev.* **2013**, *42*, 548. (b) Xiang, Z.; Cao, D. *J. Mater. Chem. A* **2013**, *1*, 2691.

(19) Kandambeth, S.; Mallick, A.; Lukose, B.; Mane, M. V.; Heine, T.; Banerjee, R. *J. Am. Chem. Soc.* **2012**, *134*, 19524.

(20) Chandra, S.; Kundu, T.; Kandambeth, S.; Babarao, R.; Marathe, Y.; Kunjir, S. M.; Banerjee, R. *J. Am. Chem. Soc.* **2014**, *136*, 6570.

(21) (a) Farha, O. K.; Spokoyny, A. M.; Hauser, B. G.; Bae, Y.-S.; Brown, S. E.; Snurr, R. Q.; Mirkin, C. A.; Hupp, J. T. *Chem. Mater.* **2009**, *21*, 3033. (b) Li, G.; Wang, Z. *J. Phys. Chem. C* **2013**, *117*, 24428.

(22) Rao, K. V.; Haldar, R.; Kulkarni, C.; Maji, T. K.; George, S. J. *Chem. Mater.* **2012**, *24*, 969.

(23) Trewin, A.; Cooper, A. I. *CrystEngComm* **2009**, *11*, 1819.

(24) Aany Sofia, L. T.; Krishnan, A.; Sankar, M.; Kala Raj, N. K.; Manikandan, P.; Rajamohanan, P. R.; Ajithkumar, T. G. *J. Phys. Chem. C* **2009**, *113*, 21114.

(25) Craven, B. M.; McMullan, R. K.; Bell, J. D.; Freeman, H. C. *Acta Crystallogr., Sect. B* **1977**, *33*, 2585.

DOI: 10.1021/ja511389q
J. Am. Chem. Soc. 2015, 137, 913−918